EFFECTS OF LOAD POINT LOCATION ON THE INSTABILITY AND NONLINEAR BEHAVIOUR OF I, CHANNEL, AND ZEE SHAPED BEAMS

By Akio HASEGAWA*, NAVEED Anwar** and DELLELEGNE Teshome***

The effects due to an arbitrary location of the load point on the buckling and post-buckling behaviour of elastic thin-walled beams are investigated. The governing differential equations and the corresponding stiffness matrices are derived, based on the virtual work equation of linearized finite displacement. Numerical examples are given to investigate the behaviour of I, channel and zee shaped beams. Location of load point greatly affects the post-buckling behaviour as well as the buckling loads. Although zee and channel sections show a large reserve strength as compared with I-section, this reserve strength corresponds to fairly large stresses and displacements.

Keywords : lateral instability, nonlinear behaviour, load point location, I-shape, channel-shape, zee-shape, FEM

1. INTRODUCTION

The design of steel members is often governed by the stability requirements rather than the material strength requirements. This is specially true for thin-walled beams having comparatively smaller stiffness in the lateral direction. When such beams are subjected to in-plane loads, they tend to buckle in the out-of-plane direction by a combination of lateral and torsional effects. This type of buckling normally referred to as lateral-torsional buckling greatly reduces the load carrying capacity of slender beams.

The lateral-torsional buckling load is affected by the shape and proportion of the cross-section, length between lateral supports, loading and boundary conditions. Another factor which affects the lateral-torsional buckling behaviour of thin-walled beams is the level of loading point with respect to the shear centre as shown in **Fig. 1**. It is clearly seen, for an example, that a load applied at the top flange of a section will produce additional torsional effects after some rotation of the cross-section, and thus reduce the stiffness of the beam. The effect of these parameters on the lateral instability of doubly-symmetric and mono-symmetric I-sections has been investigated in the past by many researchers[1]~[4]. However investigation into the behaviour of un-symmetric section such as zee and channel shapes has received much less attention[5],[6].
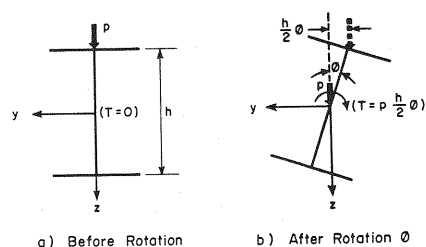

a) Before Rotation   b) After Rotation Ø

Fig. 1 Effect of Load Point Location.

* Member of JSCE, Dr. Eng., Professor, Department of Civil Engineering, University of Tokyo (Bunkyo-ku, Tokyo 113, Japan)
** M. Eng., Managing Partner, Nam Associated Consultants (Model Town, Lahore, Pakistan)
*** Dr. Eng., Assistant Professor, Department of Civil Engineering, University of Addis Ababa, Addis Ababa, Ethiopia, formerly graduate student of University of Tokyo.

Since the availability of extensive computing facilities, many formulations based on the finite element procedures have been proposed for the nonlinear analysis of thin-walled structures, including the lateral-torsional buckling of beams[7]~[11]. However, in these formulations, the effects due to the location of load point have not been considered explicitly. The aim of the present study is therefore to incorporate the additional effects due to the arbitrary location of the load points into the existing formulation[10] for the out-of-plane instability of general elastic thin-walled beams. It is further intended to specialize this treatment to study the behaviour of channel and zee section beams and to compare it to that of I-section.

2. THEORETICAL FORMULATION

Consider a general thin-walled member subjected to nodal forces, and also subjected to distributed loads along the span as shown in **Fig. 2**, in which x, y, z are the right hand cartesian coordinates and u_c is the axial displacement of the centroid, v_s, w_s are the displacements of the shear centre in y, z directions of principal axes respectively, and ϕ is the rotation of the section about the shear centre. The rigorous expressions for the displacements u, v and w of an arbitrary point across the section are given[10] as,

$$\left.\begin{array}{l} u=u_c-v'_s(y\cos\phi-z\sin\phi)-w'_s(z\cos\phi+y\sin\phi)-\omega\phi' \\ v=v_s-(y-y_s)(1-\cos\phi)-(z-z_s)\sin\phi \\ w=w_s+(y-y_s)\sin\phi-(z-z_s)(1-\cos\phi) \end{array}\right\} \quad\cdots\cdots\cdots\cdots\cdots (1\cdot a\sim c)$$

It is noted that all the displacement components in Eq. (1) are regarded as incremental quantities in subsequent formulations. It is also noted that all the notations to appear in this paper are the same as in Ref. 10), unless otherwise specifically mentioned.

It is important to note that the uniform loads and the nodal forces are applied at arbitrary points P_1 (y_p, z_s) and $P_2(y_s, z_p)$ as shown in **Fig. 3** and not at the shear centre. It is assumed that the load points move with the cross-section during deformation, but the direction of load application does not change, as has been shown in **Fig. 1**. In such circumstances, the displacements of the load points are of considerable importance and can be obtained by substituting the coordinates of P_1 and P_2 into the general displacement field of Eq. (1), and neglecting the third and higher order terms as

$$\left.\begin{array}{l} v_p=v_s-(y_p-y_s)(1-\cos\phi)-(z_s-z_s)\sin\phi\doteqdot v_s-1/2(y_p-y_s)\phi^2\equiv v^L+v^{NL} \quad \text{at } P_1 \\ w_p=w_s+(y_s-y_s)\sin\phi-(z_p-z_s)(1-\cos\phi)\doteqdot w_s-1/2(z_p-z_s)\phi^2\equiv w^L+w^{NL} \quad \text{at } P_2 \end{array}\right\} \cdots (2\cdot a, b)$$

It can be observed from the above equations that the displacement field on the load points contains linear (L) as well as nonlinear (NL) parts and can be used to evaluate the additional effects due to the location of load points on the governing equations. The general virtual work equation of such a beam in linearized finite displacement after ignoring third and higher order terms can be obtained as

$$\int_V(\sigma^0_{ij}\delta e^{NL}_{ij}+\sigma^L_{ij}\delta e^L_{ij})dV-\int_L(p^0_i\delta u^{NL}_i+p_i\delta u^L_i)dx-[F^0_{lk}\delta u^{NL}_{lk}+F_{lk}\delta u^L_{lk}]_{k=i,j}=0 \cdots\cdots\cdots\cdots\cdots (3)$$
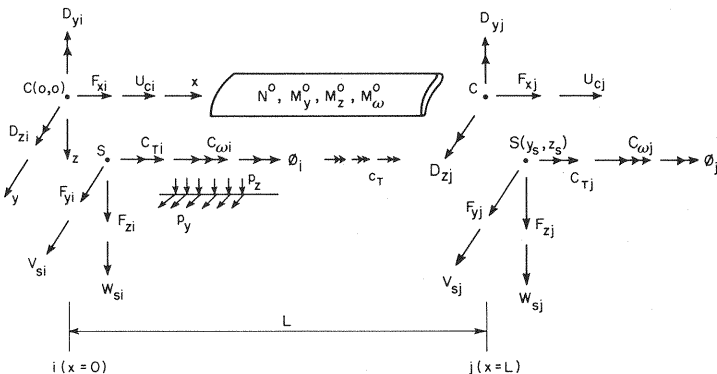

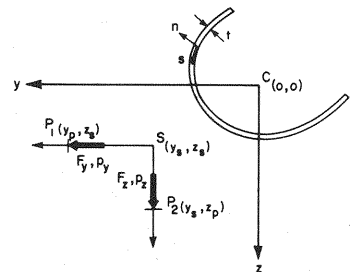Fig. 2 Generalized Forces and Displacements.

Fig. 3 Location of Load Points on the Cross Section.

in a similar way as derived in Ref. 10), where superscript (0) indicates the quantities defined at the reference state and σ_{ij}, p_i, F_i, u_i and e_{ij} are incremental quantities measured from the reference state. The normal stress σ_{xx}^0 at the reference state is defined in terms of the stress resultants, which are the internal axial force N^0, bending moments M_y^0, M_z^0 and warping moment M_ω^0, all of which are assumed constant over the element length, as

$$\sigma_{xx}^0 = \frac{N^0}{A} + \left(\frac{M_y^0}{I_{yy}}\right)y + \left(\frac{M_z^0}{I_{zz}}\right)z + \left(\frac{M_\omega^0}{I_{\omega\omega}}\right)\omega \cdots\cdots\cdots (4)$$

with reference to the principal axes, where

$$A = \int_A da \qquad I_{yy} = \int_A y^2 da \qquad I_{zz} = \int_A z^2 da \qquad I_{\omega\omega} = \int_A \omega^2 da \cdots\cdots (5 \cdot a \sim d)$$

Equation (4) and the non-zero stress and strain components obtainable from Eq. (1) by making use of the Green's strain-displacement and linear constitutive relations, together with the displacement field on the load points of Eq. (2) are substituted into the virtual work equation (3) of linearized finite displacements (see Ref. 10) for details) and, through the variational procedures, the governing differential equations are obtained as,

$$
\left.
\begin{aligned}
&EA u_c'' = p_x \\
&EI_{yy} v_s^{(4)} - N^0 v_s'' + (-z_s N^0 + M_z^0)\phi'' = p_y \\
&EI_{zz} w_s^{(4)} - N^0 w_s'' + (y_s N^0 - M_y^0)\phi'' = p_z \\
&EI_{\omega\omega}\phi^{(4)} - GJ\phi'' + (-z_s N^0 + M_z^0)v_s'' + (y_s N^0 - M_y^0)w_s'' \\
&\quad - (r_s^2 N^0 + \beta_y M_y^0 + \beta_z M_z^0 + \beta_\omega M_\omega^0)\phi'' + \{p_y^0(y_p - y_s) + p_z^0(z_p - z_s)\}\phi = c_T
\end{aligned}
\right\} \cdots\cdots\cdots (6 \cdot a \sim d)
$$

with the associated boundary conditions at $x = 0$ and L ($k = i$ and j) as,

$$
\left.
\begin{aligned}
&u_c = u_{ck} && \text{or} && n_x EA u_c' = F_{xk} \\
&v_s = v_{sk} && \text{or} && n_x[-EI_{yy}v_s''' + N^0 v_s' + (z_s N^0 - M_z^0)\phi'] = F_{yk} \\
&-v_s' = -v_{sk}' && \text{or} && n_x[-EI_{yy}v_s'' - M_z^0\phi] = D_{yk} \\
&w_s = w_{sk} && \text{or} && n_x[-EI_{zz}w_s''' + N^0 w_s' + (-y_s N^0 + M_y^0)\phi'] = F_{zk} \\
&-w_s' = -w_{sk}' && \text{or} && n_x[-EI_{zz}w_s'' + M_y^0\phi] = D_{zk} \\
&\phi = \phi_k && \text{or} && n_x[-(EI_{\omega\omega}\phi''' - GJ\phi') + z_s N^0 v_s' - y_s N^0 w_s' \\
& && && \quad + (r_s^2 N^0 + \beta_y M_y^0 + \beta_z M_z^0 + \beta_\omega M_\omega^0)\phi'] \\
& && && \quad + \{F_{yk}^0(y_p - y_s) + F_{zk}^0(z_p - z_s)\}\phi_k = C_{Tk} \\
&-\phi' = -\phi_k' && \text{or} && n_x[-EI_{\omega\omega}\phi''] = C_{\omega k}
\end{aligned}
\right\} \cdots\cdots\cdots (7 \cdot a \sim g)
$$

where $n_x = -1$ at $x = 0$, $n_x = 1$ at $x = L$, and

$$
\left.
\begin{aligned}
&J = \int_A \Theta^2 da \qquad r_s^2 = [I_{yy} + I_{zz} + A(y_s^2 + z_s^2)]/A \qquad \beta_y = -2 y_s + (1/I_{yy})\int_A (y^2 + z^2)y da \\
&\beta_z = -2 z_s + (1/I_{zz})\int_A (y^2 + z^2)z da \qquad \beta_\omega = (1/I_{\omega\omega})\int_A (y^2 + z^2)\omega da
\end{aligned}
\right\} \cdots\cdots (8 \cdot a \sim e)
$$

These differential equations are important from a theoretical point of view and for obtaining the analytical solutions. However, for general loading and boundary conditions, these equations are difficult to solve and a finite element procedure in the form of stiffness equations is more useful from a computational point of view.

3.   FINITE ELEMENT MODEL

In a similar procedure as described in Ref. 10) for warping beams and Ref. 12) for non-warping beams with the use of the well-known Hermite interpolation polynomials, the general stiffness equation of order 14×14 for warping beams[10] or of order 12×12 for non-warping beams[12] subjected to loads applied at arbitrary points across the section is obtained as

$$F = Kd - F_0 \quad \text{i. e.} \quad \begin{Bmatrix} F_x \\ F_y \\ F_z \\ T \end{Bmatrix} = \begin{bmatrix} K_{11} & & & \text{sym.} \\ 0 & K_{22} & & \\ 0 & 0 & K_{33} & \\ 0 & K_{42} & K_{43} & (K_{44}+K_a+K_b) \end{bmatrix} \begin{Bmatrix} U \\ V \\ W \\ \Phi \end{Bmatrix} - \begin{Bmatrix} F_{0x} \\ F_{0y} \\ F_{0z} \\ T_0 \end{Bmatrix} \quad \text{(9·a, b)}$$

in which the block matrices K_{ij} $(i, j=1{\sim}4)$ have been given in Refs. 10), 12).

There are two additional block matrices K_a and K_b, newly introduced in this study in Eq. (9). Matrix K_a expressed as

$$K_a = [p_y^0(y_p - y_s) + p_z^0(z_p - z_s)]\overline{K}_a \quad \text{(10)}$$

accounts for the additional effects due to the location of uniformly distributed loads p_y and p_z applied away from the shear centre, defined at the reference state. The elements of matrix $\overline{K}_a$ for warping beams can be obtained as,

$$\overline{K}_a = \int_L BB^T dx = \begin{bmatrix} 13L/35 & & \text{sym.} & \\ -11L^2/210 & L^3/105 & & \\ 9L/70 & -13L^2/420 & 13L/35 & \\ 13L^2/420 & -L^3/140 & 11L^2/210 & L^3/105 \end{bmatrix} \quad \text{(11)}$$

where B is the well-known third order interpolation vector as given in Ref. 10). Matrix K_b expressed as

$$K_b = [F_{yk}^0(y_p - y_s) + F_{zk}^0(z_p - z_s)]_{k=i,j}\overline{K}_b \quad \text{(12)}$$

accounts for the additional effects due to the location of nodal forces F_y and F_z applied away from the shear centre, defined at the reference state, where $[A]_{k=i,j}$ indicates the sum of A defined at $k=i$ and $k=j$, and Matrix $\overline{K}_b$ for warping beams is given as

$$\overline{K}_b = BB^T = \begin{bmatrix} \delta_{ki} & 0 & 0 & 0 \\ 0 & 0 & 0 & 0 \\ 0 & 0 & \delta_{kj} & 0 \\ 0 & 0 & 0 & 0 \end{bmatrix} \quad \text{(13)}$$

where, δ_{ki} and δ_{kj} are the well-known symbol of Kronecker's delta. The vector F_0 in Eq. (9) is the equivalent nodal force vector as given by

$$F_0 = \langle F_{0x}, F_{0y}, F_{0z}, T_0 \rangle^T \quad \text{(14)}$$

where,

$$F_{0x} = p_x \int_L A^T dx \qquad F_{0y} = p_y \int_L B^T dx \qquad F_{0z} = p_z \int_L B^T dx \qquad T_0 = c_\tau \int_L B^T dx \quad \text{(15·a~d)}$$

for warping beams, in which A is the well-known first order interpolation vector as given in Ref. 10), and then,

$$\int_L A^T dx = \left\langle \frac{L}{2}, \frac{L}{2} \right\rangle, \quad \int_L B^T dx = \left\langle \frac{L}{2}, \frac{L^2}{12}, \frac{L}{2}, -\frac{L^2}{12} \right\rangle \quad \text{(16·a, b)}$$

For beams having non-warping cross-sectional shapes such as box and tubed sections, the expressions of $\overline{K}_a$, $\overline{K}_b$ and T_0 are different from Eqs. (11), (13), (15·d), respectively, and can be obtained through a similar procedure as for warping beams as

$$\overline{K}_a = \int_L AA^T dx = \begin{bmatrix} L/3 & L/6 \\ L/6 & L/3 \end{bmatrix} \qquad \overline{K}_b = AA^T = \begin{bmatrix} \delta_{ki} & 0 \\ 0 & \delta_{kj} \end{bmatrix} \quad \text{(17·a, b)}$$

in place of Eqs. (11) and (13), and

$$F_{0x} = p_x \int_L A^T dx \qquad F_{0y} = p_y \int_L B^T dx \qquad F_{0z} = p_z \int_L B^T dx \qquad T_0 = c_\tau \int_L A^T dx \quad \text{(18·a~d)}$$

in place of Eq. (15).

Equation (9) represents the tangent stiffness equation of a general thin-walled beam and includes the additional effects due to the arbitrary location of uniformly distributed and/or nodal forces applied away from the shear centre. The additional matrices K_a, K_b and F_0 which have not appeared in Refs. 10), 12)

can be incorporated into the nonlinear analysis scheme for elastic thin-walled frames and beams[11].

4. LATERAL BUCKLING

Thin-walled beams which are not continuously supported in lateral direction may fail due to a combination of lateral and torsional deformations known as lateral buckling. Consider a simply supported beam placed on the $x-z$ plane with $y_s = 0$, subjected to axial compressive force P^0 and bending moment M^0 (resulting either from distributed loads or concentrated forces, being considered constant for any particular element). The stress resultants at the reference state therefore are given as

$$N^0 = -P^0 \qquad M_y^0 = 0 \qquad M_z^0 = M^0 \qquad M_\omega^0 = 0 \quad\cdots\cdots\cdots\cdots\cdots\cdots\cdots\cdots\cdots\cdots\cdots\cdots (19\cdot a\sim d)$$

in which P^0 is taken positive for compressive force. For this particular case, the governing stiffness equation of order 8×8 for warping beams and 6×6 for non-warping beams can be extracted from the general expression of Eq. (9) as

$$F = [K_E + K_G]d \quad \text{i. e.} \quad \begin{Bmatrix} F_y \\ T \end{Bmatrix} = \begin{bmatrix} K_{22} & K_{42} \\ K_{42} & (K_{44} + K_a + K_b) \end{bmatrix} \begin{Bmatrix} V \\ \Phi \end{Bmatrix} \cdots\cdots\cdots\cdots\cdots\cdots (20)$$

where K_E and K_G are the small displacement and geometric stiffness matrices, respectively, given for warping beams as,

$$K_E = \begin{bmatrix} (EI_{yy}/L^3)K_1 & 0 \\ 0 & (EI_{\omega\omega}/L^3)K_1 + (GJ/L)K_2 \end{bmatrix} \cdots\cdots\cdots\cdots\cdots\cdots\cdots\cdots (21)$$

and,

$$K_G = \frac{1}{L}\begin{bmatrix} 0 & M^0 K_3^T \\ M^0 K_3 & (\beta_z M^0 K_2 + K_a + K_b) \end{bmatrix} - \frac{P^0}{L}\begin{bmatrix} K_2 & z_s K_2 \\ z_s K_2 & r_s^2 K_2 \end{bmatrix} \cdots\cdots\cdots\cdots\cdots (22)$$

in which $K_1 \sim K_3$ are given in Ref. 10), and the corresponding expressions for non-warping beams can be obtained through Ref. 12).

At the critical condition, more than one equilibrium state are possible without any additional load being applied $(F = 0)$ and then the non-trivial solution of Eq. (20) may exist as,

$$[K_E + \lambda \overline{K}_G]d = 0 \cdots\cdots\cdots\cdots\cdots\cdots\cdots\cdots\cdots\cdots\cdots\cdots\cdots\cdots\cdots\cdots\cdots\cdots\cdots\cdots\cdots\cdots\cdots\cdots\cdots\cdots (23)$$

where $\lambda \overline{K}_G = K_G$ and λ represents the eigenvalue usually expressed by M^0 or P^0 for the problem of lateral buckling of beams subjected to in-plane loading, including the effects due to the location of load points being away from the shear centre. It is noted in the eigenvalue equation (23) that matrix K_E is symmetric and positive definite whereas K_G is symmetric but semi-definite (singular for $P^0 = 0$). For this case the smallest eigenvalue which gives the critical load parameter may be found using the Householder QR-inverse iteration method[13].

5. NUMERICAL EXAMPLES AND DISCUSSIONS OF RESULTS

(1) Cross-sectional properties

The behaviour of channel and zee section members as shown in Fig. 4, which are commonly used as purlins and beams in construction of steel structures, is more complex to analyse than that of I-sections, due to the fact that both of these sections are not doubly symmetric. In the case of channel section the shear centre does not coincide with the centroid and thus produces additional torsional disturbance due to a possible eccentricity of loadings whereas for zee section the principal axes are inclined with respect to the web axis, resulting in additional complications. The so-called Wagner effects on the instability phe-
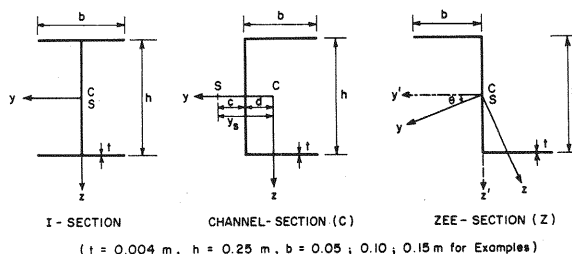

I - SECTION   CHANNEL- SECTION (C)   ZEE- SECTION (Z)

(t = 0.004 m, h = 0.25 m, b = 0.05 ; 0.10 ; 0.15 m for Examples)

Fig. 4   Cross-Section Types Used for Analysis.

nomena can also be taken into account by the second order cross-sectional properties such as the mono-symmetrical properties β_y, β_z and asymmetrical property β_ω as defined in Eq. (8). A derivation of these sectional properties with respect to the principal axes has been carried out in this study for these shapes and the resulting formulas are given in APPENDIX. The absolute values of these properties greatly affect the stability and the large displacement behaviour of beams, specially at high load levels when the value of the internal stress resultants becomes large.

(2) Beam model for numerical examples

The theoretical formulation presented above is now applied to a simply supported beam as shown in Fig. 5. A span length ($L=6.0$ m) is used for different cross-section types i. e. I, C and Z shapes, having the same dimensions. Three different values of flange widths ($b=0.05$ m, 0.1 and 0.15 m) are used for each section type whereas constant height ($h=0.25$ m) and wall thickness ($t=0.004$ m) are used for all beams. For each section type and flange width, a uniformly distributed load is applied at the top flange level (TF), at the shear centre level (SC) and at the bottom flange level (BF) as shown in Fig. 5. Therefore a total of 27 cases have been examined, where each case is designated by the order of section shape (I, C or Z), flange width in cm (05, 10 or 15), followed by the point of load application (TF, SC or BF) such as I 05 TF, C 10 SC and so on. The original load is considered to be applied through the web axis and thus is decomposed into appropriate components for the purpose of analysis. The beam is modelled by eight elements for the whole beam which were found to be sufficient by the convergence study and was analysed by using 90 incremental load steps which resulted in a load level of approximately 2. 3 times the buckling load of the corresponding I-section beams with acceptable accuracy. The nonlinear load-displacement path for each beam was traced by using the finite element procedure given in Ref. 11).

(3) Buckling and nonlinear load-displacement behaviour

Firstly for the verifications of the present formulation for the effects of point of load application, the lateral buckling loads obtained by the present analysis for I-section beams are compared with the semi-analytical solutions given by Timoshenko[2] and Table 1 shows that the results were found to be in close agreement for different locations of load point and for different values of flange width. It may be noted that the present results are considered more reliable than those of Ref. 2) which only gave approximate solutions.

Another way of obtaining the critical loads is to observe the load displacement curve for lateral displacement and a point where small increment in load causes large lateral displacement may be regarded as the critical buckling load. The initial imperfection is given in the load-displacement analysis of I-section beams by a mid-span concentrated lateral load which produces the initial displacement of $0.001 L$ for SC and BF beams and $0.002 L$ for TF beams at the initial stage. It is observed that the value obtained from the curves closely corresponds to the bifurcation load obtained by eigenvalue analysis for I-section beams (Fig. 6(a)). The small difference between the graphical value and the numerical value is partly due to the
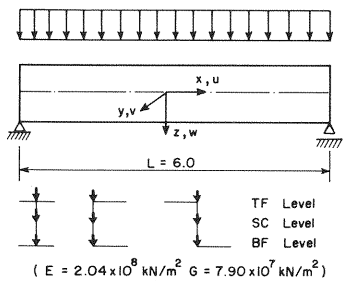

Fig. 5   Beam Model used for Analysis.

Table 1   Comparison of Buckling Loads.

Section	b/h	Load Location	$P_{cr}(a)$ kN/m	$P_{cr}(p)$ kN/m	% Diff.
I 05	0.2	Top Flange	0.37	0.38	− 2.7
		Shear Centre	0.45	0.45	0.0
		Bottom Flange	0.53	0.52	+ 1.8
I 10	0.4	Top Flange	1.34	1.34	0.0
		Shear Centre	1.81	1.80	+ 0.6
		Bottom Flange	2.46	2.43	− 1.2
I 15	0.6	Top Flange	3.31	3.36	− 1.5
		Shear Centre	4.82	4.85	− 0.6
		Bottom Flange	7.16	7.04	+ 1.6

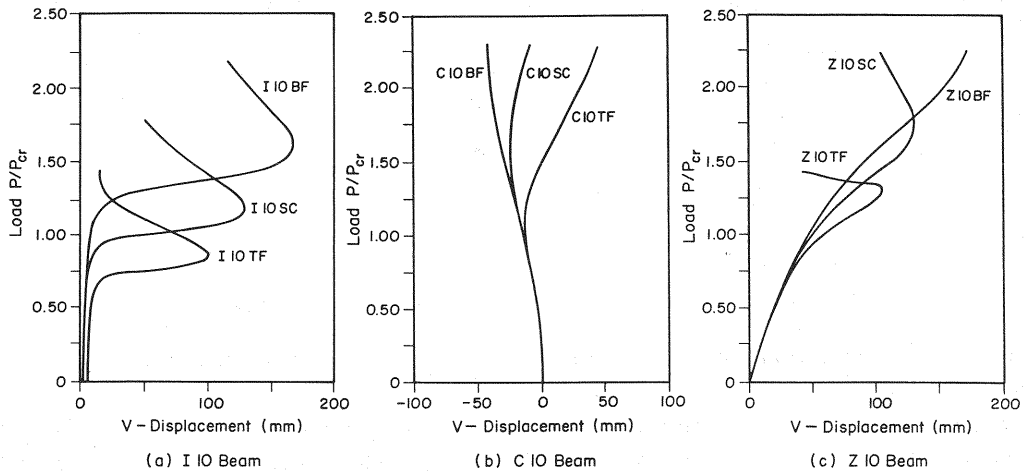Remarks : $P_{cr}(a)$ = Ref. 2 , $P_{cr}(p)$ = Present Study

Fig. 6   Effects of Load Point Location on Load-Displacement Curves.

initial imperfections used in the nonlinear analysis to avoid singularity of the tangent stiffness matrix at the bifurcation point. However, for C and Z section beams, no sudden increase in displacement was observed and hence they do not exhibit a pronounced buckling phenomenon (Fig. 6(b), (c)). This is due to the simultaneous presence of lateral load component for zee section arising from the inclination of the principal axis and due to the presence of torsional moment in channel section arising from the eccentricity of the load from the shear centre and also due to the distance between shear centre and the centroid which gives rise to additional torsional disturbances. It may be noted that, for the purpose of better comparison, the load on the vertical axis in all figures has been normalized with respect to the critical buckling load of the corresponding I-section beam for the case of loading applied at the shear centre. It is also noted that all the displacements plotted in figures throughout this paper indicates the value at the mid-span of the beam, with displacement v for the shear center of C-section and for the direction y' (not principal axis) perpendicular to the web for Z-section (see Fig. 4).

It is observed from a comparison of load displacement behaviour of different shaped beams that C-Section undergoes the largest rotations even at low load levels (Fig. 7(a)) due to the presence of torsional moment induced by the eccentricity of the load from the shear centre, whereas Z-section shows the greatest lateral displacement due to the presence of large lateral load component (Fig. 7(b)). Although C and Z sections do not exhibit any critical buckling phenomena, and seem to give a large reserve strength, the maximum stress at these load levels far exceeds the yield strength of normal steel. It is also noted that
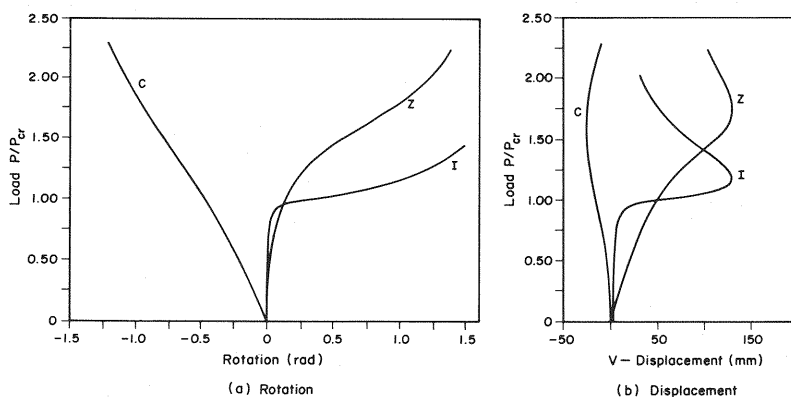

Fig. 7   Comparisons of Rotation and Displacement for 10 SC Beam.

(a) I – Section   (b) C – Section   (c) Z – Section
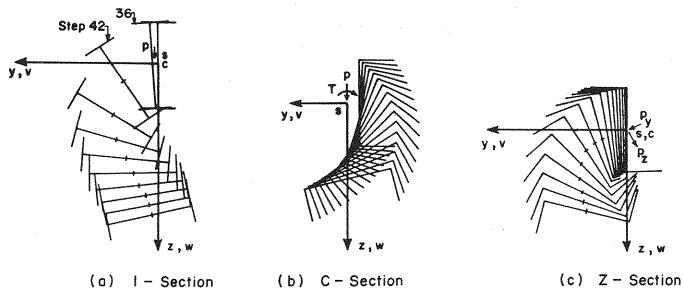
Fig. 8   Deformed Configurations of Cross Sections for 10 SC Beam.

this reserve strength is available at fairly large displacements, which are not normally allowed in design practice. Fig. 8 shows the actual rotation and displacement of the coss-section, which have been plotted after every six load steps. It is observed that no "sudden" displacement of Z or C section occurs as in the case of I-section, which buckles suddenly between load step 36 and 42. It should also be noted that all the sections undergo fairly large rotation at higher load level, which completely changes the direction of applied loads (that is oriented in the global axis) with respect to the local member axis. The "snapback" or reduction in lateral displacement v can also be seen with a greater clarity, which may seem unrealistic at first glance in the load displacement curves.

The value of lateral buckling load is greatly affected by the flange width i. e. b/h ratio, and it increases sharply as the flange becomes wider, as clearly indicated by Table 1. The load displacement behavior of I-sections for different flange widths (b/h ratio) is nearly similar as can be seen from Fig. 9 (a), except for the fact that the normalizing critical load is different in each case. The behavior of zee and channel sections is, however, significantly affected by the b/h ratio due to the fact that in both cases the basic load components are dependent upon the proportions of the cross-section which in turn are affected by the flange width to web height ratio. For wide flange C-sections, the torsional moment becomes large due to a bigger value of y_s and may completely change the direction and magnitude of displacements (Fig. 9 (b)). Similarly the direction of principal axes in the case of Z-section depends upon the b/h ratio, which affects the direction and magnitude of p_y and p_z which in turn affect the absolute and relative values of displacements v and w, as shown in Fig. 9 (c).

It can be seen from Fig. 1 and from Eq. (9) that any load which is applied at a distance from the shear cetre (in line with shear centre axis) increases or decreases the stiffness of a member. In other words, the same load, when applied at different levels along the shear centre axis, will produce different load-displacement curve, and will result in different values of buckling load. This phenomena are clearly
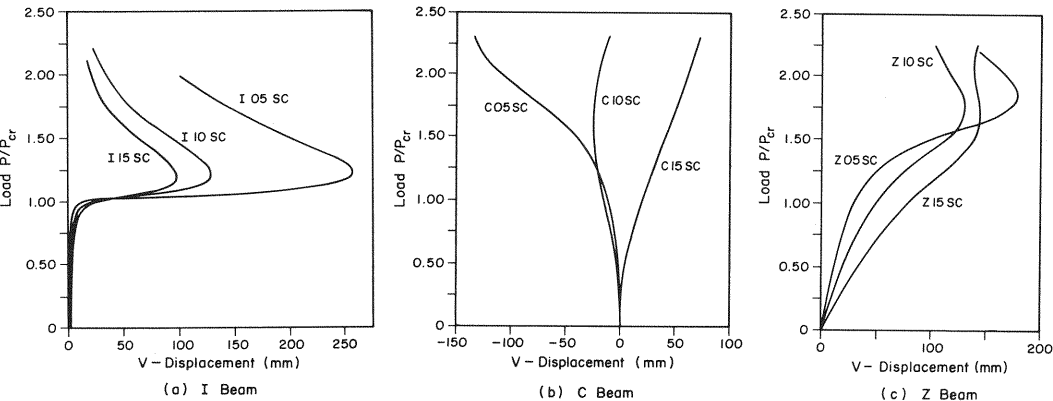

(a) I Beam   (b) C Beam   (c) Z Beam

Fig. 9   Effects of Flange Width on Load-Displacement Curves (Shear Center Loading).

demonstrated by this study in **Fig. 6** and by **Table 1**. It is important to note in **Fig. 6**(a) that the difference in displacements for a given load level due to the change in the location of load only becomes significant after buckling of I-sections, and there is practically no difference in behaviour before buckling, except for the fact that buckling load itself depends upon load location. For channel and zee sections, which start to undergo large rotations and displacements even at low load levels, load location has a greater effect on the load-displacement curve (**Fig. 6**(b), (c)). The load carrying capacity of these sections, for a prescribed value of displacement, increases appreciably when load is applied at the bottom flange, in which case the design based on shear centre loading is conservative, whereas the shear centre loading assumption gives unsafe deflections and stresses when actual load is applied at the top flange.

6. CONCLUSIONS

The effects due to an arbitrary location of the load point on the buckling and post-buckling behaviour of thin-walled beams have been investigated. The governing differential equations and the corresponding stiffness matrix have been derived, based on the virtual work equation of linearized finite displacement. This extended stiffness matrix has been incorporated into the finite element model of Hasegawa et al. [11] to trace the nonlinear displacement path. A reduced stiffness matrix has also been derived for the evaluation of buckling loads. The formulation has been used to numerically investigate the elastic finite displacement behaviour of I, channel and zee shaped beams. The following conclusions can be drawn from the computational results obtained in this study.

(1)　The finite element formulation with the reduced stiffness matrix presented in this study has given excellent agreement with the available semi-analytical solutions of lateral buckling loads for the effects due to the different locations of load point.

(2)　Location of load point greatly affects not only the buckling loads, but also the finite displacement behaviour of all the beams used in this study.

(3)　Although zee and channel sections show a large reserve strength as compared with I-section, this reserve strength corresponds to fairly large stresses and displacements.

(4)　Flange width to web height ratio has a much greater effect on the load displacement behaviour of zee and channel sections than on that of I-section.

APPENDIX : SECTION PROPERTIES

The second order cross sectional properties along with torsional properties are given below for I, channel and zee sections as shown in **Fig. 4** with y, z axes being principal axes.

1) I-SECTION

$$I_{\omega\omega}=\frac{b^3 h^2 t}{24} \qquad J=\frac{t^3}{3}(2\,b+h) \qquad r_s^2=\frac{(I_{yy}+I_{zz})}{A}$$

$$\beta_y=0 \qquad\qquad \beta_z=0 \qquad\qquad \beta_\omega=0$$

2) C-SECTION

$$c=\frac{3\,b^2}{(6\,b+h)} \qquad d=\frac{b^2}{(2\,b+h)} \qquad y_s=c+d$$

$$I_{\omega\omega}=\frac{tb^3 h^2(3\,b+2\,h)}{12(6\,b+h)} \qquad J=\frac{t^3}{3}(2\,b+h) \qquad r_s^2=\frac{(I_{yy}+I_{zz}+Ay_s^2)}{A}$$

$$\beta_y=-2\,y_s+\frac{1}{I_{yy}}\left\{\frac{b\,t}{2}\left[(-b^3+4\,b^2 d-6\,bd^2+4\,d^3)+\frac{h^2}{2}(-b+2\,d)\right]+\frac{hd\,t}{12}(12\,d^2+h^2)\right\}$$

$$\beta_z=0 \qquad\qquad \beta_\omega=0$$

3) Z-SECTION

$$I_{\omega\omega}=\frac{tb^3h^2(b+2h)}{12(2b+h)} \qquad J=\frac{t^3}{3}(2b+h) \qquad r_s^2=\frac{(I_{yy}+I_{zz})}{A}$$

$$\beta_y=0 \qquad \beta_z=0 \qquad \beta_\omega=\frac{b^2ht}{24(2b+h)I_{\omega\omega}}[4b^3+6b^2h+2h^3]$$

REFERENCES

1) Vlasov, V. : Thin-Walled Elastic Beams, Israel Program for Scientific Translation, Jerusalem, 1961.

2) Timoshenko, S. P. and Gere, J. M. : Theory of Elastic Stability, 2nd Edition, McGraw-Hill Inc., 1961.

3) Nethercot, D. A. and Rockey, K. C. : A Unified Approach to Elastic Lateral Buckling of Beams, the Structural Engineer, Vol. 49, No. 7, pp. 321-330, July, 1971.

4) Anderson, J. M. and Trahair, N. S. : Stability of Monosymmetric Beams and Cantilevers, Journal of the Structural Division, ASCE, Vol. 98, No. ST-1, pp. 269-286, Jan., 1972.

5) Hill, H. N. : Lateral Buckling of Channel and Zee Beams, Transactions of ASCE, Vol. 119, Paper No. 2700, pp. 829-841, 1954.

6) Murray, N. W. and Lau, Y. C. : The Behaviour of Channel Cantilever Under Combined Bending and Torsional Loads, Thin Walled Structures 1, Applied Sciences Publications Ltd., England, pp. 55-74, 1983.

7) Chan, S. L. and Kitipornchai, S. : Geometric Nonlinear Analysis of Asymmetric Thin-Walled Beam-Columns, Engineering Structures, Vol. 9, No. 4, pp. 243-254, Oct., 1987.

8) Meek, J. L. and Tan, H. S. : Large Deflection and Post Buckling Analysis of Two and Three Dimensional Spatial Frames, Research Report No. CE49, Department of Civil Engineering, University of Queensland, Australia, Dec., 1983.

9) Bazant, Z. P. and Nimeiri, E. L. : Large Deflection Spatial Buckling of Thin-Walled Beams and Frames, Journal of the Engineering Mechanics Division, ASCE, Vol. 99, No. EM-6, pp. 1259-1281, Dec., 1973.

10) Hasegawa, A., Liyanage, K., Ikeda, T. and Nishino, F. : A Concise and Explicit Formulation of Out-of-Plane Instability of Thin-Walled Members, Structural Eng. ／Earthquake Eng., JSCE, Vol. 2, No. 1, pp. 57s-65s (Proc. JSCE, No. 356／I -3), April, 1985.
Closure to a Discussion for the above paper by Usuki, S., Vol. 3, No. 1, pp. 203s-205s (Proc. JSCE, No. 368／I -5), April 1986.

11) Hasegawa, A., Liyanage, K. and Nishino, F. : A Non-Iterative Nonlinear Analysis Scheme of Frames with Thin-Walled Elastic Members, Structural Eng. ／Earthquake Eng., JSCE, Vol. 4, No. 1, pp. 19s-29s (Proc. JSCE, No. 380／I -7), April, 1987.

12) Hasegawa, A., Iwakuma, T., Liyanage, K. and Nishino, F. : A Consistant Formulation of Trusses and Non-Warping Beams in Linearized Finite Displacements, Structural Eng. ／Earthquake Eng., JSCE, Vol. 3, No. 2, pp. 477s-480s (Proc. JSCE, No. 374／I -6), Oct., 1986.

13) For example, Jenning, A. : Matrix Computations for Engineers and Scientists, John Wiley & Sons, 1977.